

1 **Rainfall redistribution in subtropical Chinese forests changes over 22**  
2 **years**

3

4 **Wanjun Zhang<sup>1,2,3</sup>, Thomas Scholten<sup>3</sup>, Steffen Seitz<sup>3</sup>, Qianmei Zhang<sup>1</sup>, Guowei Chu<sup>1</sup>, Linhua**  
5 **Wang<sup>1</sup>, Xin Xiong<sup>4</sup>, Juxiu Liu<sup>1</sup>**

6

7 <sup>1</sup>Key Laboratory of Vegetation Restoration and Management of Degraded Ecosystems, South China  
8 Botanical Garden, Chinese Academy of Sciences, Guangzhou, 510650, China

9 <sup>2</sup>Key Laboratory of Urban Water Safety Discharge and Resource Utilization, Hunan University of  
10 Technology, Zhuzhou, 412007, China

11 <sup>3</sup>Soil Science and Geomorphology, Department of Geosciences, University of Tübingen, Tübingen,  
12 72070, Germany

13 <sup>4</sup>Jiangxi Provincial Key Laboratory of Carbon Neutrality and Ecosystem Carbon Sink, Lushan  
14 Botanical Garden, Jiangxi Province and Chinese Academy of Sciences, Jiujiang, 332900, China

15

16 **Correspondence:** Juxiu Liu (ljxiu@scbg.ac.cn) and Xin Xiong (xiongx@lsbg.cn)

17 **Abstract**

18         Rainfall redistribution through the vegetation canopy plays a key role in the  
19 hydrological cycle. Although there have been studies on the heterogeneous patterns of  
20 rainfall redistribution in some ecosystems, the understanding of this process in different  
21 stages of forest succession remains insufficient. Therefore, this study investigated the  
22 change tendency of rainfall redistribution and rainwater chemistry in a subtropical  
23 forest succession in South China, based on 22 years (2001–2022) of monitoring rainfall  
24 (740 valid events).

25         Results showed that at the event scale both throughfall ratio and stemflow ratio in  
26 pine forest (PF) were higher than in mixed forest (MF) and broadleaf forest (BF). At  
27 the interannual scale, throughfall and stemflow of forests experienced an initial  
28 decrease followed by a subsequent increase over the entire measurement period (except  
29 stemflow of the pine forest), which reflects the trend of open rainfall. The variability of  
30 throughfall showed an increase from MF to PF to BF, and the variability of stemflow  
31 likewise showed an increase from MF to PF to BF. Changes of throughfall and stemflow  
32 in the broadleaf forest are thus higher than those in the mixed forest and pine forest  
33 over time. Furthermore, important differences in rainwater chemistry fluxes among the  
34 three forest types were found, changing in varying order over time. On average, total  
35 nitrogen (TN) and total phosphorus (TP) fluxes of throughfall increased from BF to MF  
36 to PF, while the potassium ( $K^+$ ) flux of throughfall showed a decrease from BF to MF  
37 to PF. Stemflow chemical fluxes varied less among forest types and over time, though  
38 tree species most importantly affected varying stemflow chemistry.

39         These results show important changes in patterns of rainfall redistribution over  
40 time and that characteristic variations are driven by rainfall and forest factors. This  
41 study thus provides insight into long-term rainfall redistribution processes by linking  
42 changes in rainfall spectra with a typical subtropical forest succession sequence.

43

44 **Keywords:** throughfall, stemflow, forest types, forest meteorology, long-term study

## 45 **1 Introduction**

46 In recent years, there has been on-going concern about the potential impacts of  
47 climate change on forest ecosystems, particularly regarding rainfall input to water  
48 resources (Reynaert et al., 2020; Grossiord et al., 2017; Bruijnzeel et al., 2011;  
49 Leuzinger and Körner, 2010). Numerous studies have documented rainfall regimes and  
50 their effect on the water cycle in different regions of the world, including spatial and  
51 temporal changes in the amount, intensity, and frequency (Brasil et al., 2018; Ponette-  
52 González et al., 2010). Meanwhile, these variables in rainfall refer to the redistribution  
53 of rainfall into canopy interception, throughfall and stemflow, being important  
54 components of hydrological processes in terrestrial ecosystems (Germer et al., 2010;  
55 Levia and Frost, 2006; Loustau et al., 1992). Rainfall redistribution patterns can impact  
56 biogeochemical cycles down to soil moisture distribution, which in turn affects the  
57 activity of soil microorganisms that decompose organic matter (Tonello et al., 2021a;  
58 Junior et al., 2017; Van Stan II and Pypker, 2015). For example, Sun et al. (2023)  
59 showed that throughfall reduction significantly affects the soil carbon cycle in a  
60 subtropical forest. Therefore, understanding the roles of rainfall redistribution in  
61 woodlands is essential.

62 Rainfall redistribution, as the partitioning into interception loss, throughfall and  
63 stemflow, is an important hydrological process that regulates water and nutrient cycling  
64 in forest ecosystems. Interception loss refers to the part of the event rainfall intercepted  
65 by the canopy, accounting for about 10%–30% of gross rainfall depending on the  
66 studied forest canopy, e.g. shrub (Zhang et al., 2015), mixed broadleaf (Yan et al., 2003),  
67 or pine (Loustau et al., 1992). The remaining rainwater reaches the ground either as  
68 throughfall or stemflow. Throughfall is a critical component of rainfall redistribution,  
69 and it contributes on average to approximately 60%–90% of the gross rainfall on the  
70 floor in forests, shrubland, or cropland. (Zhang et al., 2023; Zhang et al., 2021; Brauman  
71 et al., 2010; Marin et al., 2000). Raindrops coalesce or splash on canopy leaf surfaces,  
72 generating spatially different throughfall volume and raindrop kinetic energies which  
73 can be larger or lower than that of open rainfall (Levia et al., 2019; Goebes et al., 2015).  
74 Stemflow, the water flowing bottomwards along the plant stem or trunk, often accounts  
75 for only a small proportion (0–12%) of rainfall (Niu et al., 2023; Yue et al, 2021; Llorens  
76 and Domingo 2007). Nevertheless, stemflow inputs can be important as hot spots for  
77 near-trunk soils, inducing water and nutrient enrichment and deep infiltration, but also  
78 erosion (Zhao et al., 2023; Llorens et al., 2022). It can funnel more water than open

79 rainfall on an equivalent area and contributes to 10% of the annual soil water input  
80 (Levia and Germer, 2015; Chang and Matzner, 2000). Throughfall and stemflow restrict  
81 water input to the soil layer, thereby affecting soil moisture conditions, runoff  
82 generation and water and nutrient cycling (Lian et al., 2022; Lacombe et al., 2018; Klos  
83 et al., 2014).

84 The proportions of rainfall redistribution are generally driven by meteorological  
85 conditions (e.g., rainfall amount, intensity, duration) and vegetation cover (e.g., canopy  
86 structures, tree characteristics) (Tonello et al., 2021a; Sun et al., 2018; Muzyło et al.,  
87 2012; Nanko et al., 2006). For meteorological conditions, numerous studies have  
88 documented that throughfall volume and stemflow volume increase with increasing  
89 gross rainfall and intensity (Ji et al., 2023; André et al., 2011). The ratios of throughfall  
90 and stemflow were both characterized as logarithmically increasing with rainfall,  
91 tending to be quasi-constant for heavy rainfall events (Zhang et al., 2021; Liu et al.,  
92 2019). This is also synchronously related to the gradual saturation of the canopy which  
93 limits the ratios of rainwater partitioning (Carlyle-Moses et al., 2004). Besides,  
94 differences in water volume spatially exist from place to place. The spatial variability  
95 (expressed as a coefficient of variation) of throughfall volume is generally higher for  
96 small rainfall events (< 10 mm) than for heavy rainfall events (Germer et al., 2006;  
97 Price et al., 1997).

98 Rainfall redistribution among different plant species can vary significantly due to  
99 differences in the structure and characteristics of their canopies. Specifically, key  
100 factors determining the redistribution of rainfall such as leaf area index (LAI), leaf  
101 shapes and orientations can affect the amount of intercepted loss and throughfall (Zhang  
102 et al., 2021; Goebes et al., 2015; Keim et al., 2006). The diameter at breast height (DBH),  
103 bark type and orientation of trunks/stems and branches influence the amount of  
104 stemflow (Levia et al., 2015; Livesley et al., 2014; Germer et al., 2010). For each of the  
105 rainfall partitioning fluxes, their responses to the influential predictors often show high  
106 variation. A modelling study of rainfall partitioning in China explained that throughfall  
107 was best represented by mean tilt angle (MTA), followed by DBH. Subsequently, DBH  
108 was the dominant predictor for stemflow, followed by LAI and bark texture (Zhang et  
109 al., 2023). Due to these factors, rainfall redistribution presented different degrees of  
110 spatial variability. This variability (expressed as coefficient of variation) decreased with  
111 increasing rainfall amount and intensity, consequently tending to be quasi-constant  
112 (Germer et al., 2006). Besides, at interannual scale, ratios of rainfall redistribution are

113 driven by annual canopy structures. The study of Niu et al. (2023) documented that the  
114 annual throughfall ratio gradually increased, while the annual stemflow ratio and  
115 interception loss ratio decreased with increasing thinning intensity in shrub plantations.  
116 Meanwhile, annual changes of rainfall events (amount and intensity) reinforced the time  
117 instability of throughfall spatial variability (Rodrigues et al., 2022). Overall, the  
118 rainfall-canopy interactions play a key role in rainfall redistribution processes and  
119 further affect the water cycle in many ecosystems.

120 The vegetation canopy is the functional interface between an ecosystem and  
121 atmospheric wet deposition (Van Stan II and Pypker, 2015). Leaves and trunks/stems,  
122 acting as a filter, alter rainwater chemical concentrations via leaching and depositing  
123 processes. As a result, throughfall and stemflow exhibit high chemical concentrations  
124 compared to open rainfall (Jiang et al., 2021; Zimmermann et al., 2007). For instance,  
125 in a Chinese pine plantation, the volume-weighted mean concentrations of  $\text{NH}_4^+$  and  $\text{NO}_3^-$   
126 in throughfall were significantly higher than those in open rainfall (Wang et al., 2023).  
127 Stemflow ion fluxes (e.g.,  $\text{K}^+$ ) from deciduous tree species were higher than those for  
128 evergreen tree species because of the differences in bark morphology and branch  
129 architecture (Su et al., 2019). Moreover, it is also common that throughfall and  
130 stemflow chemistry show fluctuating seasonality with the shifts in rainfall regime and  
131 leaf growth (Turpault et al., 2021; Siegert and Levia, 2014; Staelens et al., 2007). Plants  
132 mainly require N, P, K, Ca and Mg. In general, N, K and Ca are the most important  
133 inputs to a forest ecosystem, and P is the least. Phosphorus (P) is considered to be a  
134 limiting nutrient element in tropical and subtropical forests. The long-term productivity  
135 of vegetation depends on the input of atmospheric P. Besides, an increasing trend of  
136 atmospheric nitrogen (N) deposition with more frequent seasonal droughts in  
137 subtropical areas of China was reported (Zhou et al., 2011), and may inhibit the growth  
138 of plants and affect the productivity and functioning of forest ecosystems (Wu et al.,  
139 2023; Borghetti et al., 2017). Therefore, the important significance of atmospheric  
140 precipitation to an ecosystem can also be confirmed for element cycling, and canopy  
141 leaching plays an important role in the chemical cycle of forest ecosystems.

142 Although there have been studies on the spatiotemporal variability of rainfall  
143 redistribution, most of these are limited to data from short-term monitoring over several  
144 months to one-two years (Liu et al., 2019; Ziegler et al., 2009; Carlyle-Moses, 2004;  
145 Marin et al., 2000). There are few studies exceeding several years of measurements and  
146 simultaneously focusing on forest structural changes and rainwater interception

147 (Grunicke et al., 2020; Shinohara et al., 2015; Jackson, 2000). Long-term field  
148 monitoring studies are valuable to gain insight into the temporal dynamics of forest  
149 hydrological processes (Rodrigues et al., 2022; Sun et al., 2023; Levia and Frost, 2006).  
150 Such studies can also contribute to identifying patterns and trends in rainfall  
151 redistribution, which is essential for predicting the long-term effect of water resource  
152 change on forest ecosystems.

153 Therefore, in this study, we focus on the changing characteristics of throughfall  
154 and stemflow in a subtropical forest succession sequence (pine forest→mixed forest→  
155 monsoon evergreen broadleaf forest), based on long-term monitoring. Specifically, the  
156 objectives are to analyze: (1) the changes in water volume of throughfall and stemflow,  
157 and (2) the changes in water chemistry (N, P, K<sup>+</sup>) of rainfall, throughfall and stemflow  
158 among the three forests. We hypothesize that: (1) both throughfall and stemflow in the  
159 broadleaf forest are characterized by high variability compared to mixed forest and  
160 followed by pine forest, and (2) the chemical fluxes of throughfall and stemflow change  
161 over time from broadleaf forest to mixed forest to pine forest. We aim to assess the  
162 variability of forest hydrological processes from a long-term perspective to help predict  
163 future dynamic trends of water resources in subtropical forest ecosystems.

164

## 165 **2 Materials and methods**

### 166 **2.1 Study site**

167 This study was conducted at the Dinghushan Biosphere Reserve (23°09' 21" N ~  
168 23°11' 30" N, 112°30' 39" E ~ 112°33' 41" E) located in Zhaoqing City, South China.  
169 Dinghushan catchment consists of two streams both with 12 km length, which flow into  
170 the West River (the main trunk of the Pearl River). According to the Köppen-Geiger  
171 climate classification (Kottek et al., 2006), the study area belongs to tropical monsoon  
172 climate (Cwa) with pronounced wet (April-September) and dry season (October-  
173 March). The average annual temperature is 20.9 °C, and the annual rainfall and  
174 evaporation are 1900 mm and 1115 mm, respectively. Dinghushan Biosphere Reserve  
175 is covered with a complete horizontal succession series of three types of subtropical  
176 forest, which is highly representative of the region (Zhou et al., 2011). Monsoon  
177 evergreen broadleaf forest (BF) is 400 years old with typical tree species including  
178 *Castanopsis chinensis* (Spreng.) Hance, *Schima superba* Gardner & Champ.,  
179 *Cryptocarya concinna* Hance, etc. The mixed pine/broadleaf forest (MF) is a natural

180 succession with a coniferous broadleaf ratio of about 4:6, and 70–80 years old. The  
181 main broadleaf tree species are *Schima superba* Gardner & Champ., *Castanopsis*  
182 *chinensis* (Spreng.) Hance, and the coniferous species *Pinus massoniana* Lamb. The  
183 pine forest (PF) planted before 1960 belongs to the primary succession community  
184 where *Pinus massoniana* Lamb forms the only tree layer. The community composition  
185 and biodiversity are shown in Table S1.

186

## 187 **2.2 Gross rainfall, throughfall and stemflow monitoring**

188 Atmospheric rainfall data was collected at Dinghushan Automatic Meteorological  
189 Station from 2001–2022. Automatic meteorological systems were used to measure  
190 atmospheric pressure (DPA501 gas-pressure meter), temperature (HMP45D sensor),  
191 relative humidity (HMP45D sensor), rainfall (SM1-1 pluviometer) and recorded with  
192 CR1000X datalogger (America Campbell). The resolution of data recording was  $\pm 0.2$   
193 mm with a time interval of 10 min. The raw data comprised annual rainfall amounts, as  
194 well as single rainfall events with throughfall and stemflow measurements.

195 Throughfall and stemflow were collected in all three forest types and  
196 synchronously measured. Devices with cross-shaped collectors ( $1.25 \text{ m}^2$ ) attached to  
197 reservoirs (1000 L) at the bottom were used to collect throughfall. Three throughfall  
198 devices were randomly installed in each forest field (Fig. S1).

199 Half-shell plastic tubes were installed around tree trunks attached to reservoirs  
200 (1000 L) at the bottom to collect stemflow. The ratio of volume (mL) to canopy area  
201 ( $\text{cm}^2$ ) is the stemflow (mm). A total of 24 trees were selected to measure stemflow  
202 volume (Table S2). In detail, four tree species were selected in the broadleaf forest,  
203 including *Acmena acuminatissima* (Blume) Merr. et Perry (SF1), *Cryptocarya*  
204 *chinensis* (Hance) Hemsl. (SF2), *Gironniera subaequalis* Planch. (SF3), *Schima*  
205 *superba* Gardn. et Champ. (SF4), with 3 repetitions respectively. Three tree species  
206 were selected in the mixed forest, including *Castanea henryi* (Skam) Rehd. et Wils.  
207 (SF5), *Schima superba* Gardn. et Champ. (SF6), *Pinus massoniana* Lamb. (SF7), with  
208 3 repetitions respectively. In the pine forest, *Pinus massoniana* Lamb. (SF8) was  
209 selected as the monitoring subject with 3 repetitions.

210

## 211 **2.3 Rainwater chemistry measurement**

212 For the measurement of rainwater chemistry, rainwater samples were taken in 2000,

213 2010 and 2022. The samples of open rainfall, throughfall and stemflow were manually  
214 collected for every one-month period, respectively. The samples of open rainfall and  
215 throughfall were collected with three repetitions, and stemflow with four repetitions in  
216 the broadleaf forest, three repetitions in the mixed forest and three repetitions in the  
217 pine forest. In total, 792 rainwater samples (108 open rainfall, 324 throughfall and 360  
218 stemflow) were collected.

219 Rainwater samples were defrosted and filtered through 0.45  $\mu\text{m}$  polypropylene  
220 membranes. Concentrations of total nitrogen (TN) and total phosphorus (TP) were  
221 measured using an ultraviolet spectrophotometer (Lambda 25, Perkin-Elmer), and ion  
222 potassium ( $\text{K}^+$ ) was measured using an inductively coupled plasma optical emission  
223 spectrometer (Optima 2000, Perkin-Elmer). The original data of TN, TP and  $\text{K}^+$  were  
224 processed into annual flux and monthly values with the weighted average method:

$$225 \quad C = \frac{\sum C_i * V_i}{\sum V_i} \quad (1)$$

226 where  $C_i$  and  $V_i$  are the concentrations of ions ( $\text{mg L}^{-1}$ ) and water sample volume (L) in  
227 each rainfall event, respectively.

228

#### 229 **2.4 Other measurement and statistical analysis**

230 In the forests, plant density and canopy structure were measured every five years  
231 since 2000. In total, 25 plots of 20 m  $\times$  20 m (A1-A25 plots) were built on an area of  
232 1ha to survey tree density (Fig. S1). Then, 25 plots of 5 m  $\times$  5 m (B1-B25 plots) were  
233 randomly set on the A1-A25 plots to survey shrub density. Finally, 25 plots of 1 m  $\times$  1  
234 m (C1-C25 plots) were randomly set on the B1-B25 plots to survey herb density. The  
235 percentage of the surface area covered by plants to the total plot area is termed canopy  
236 coverage (%). 25 observation plots (1 m  $\times$  1 m) were selected in the 1  $\text{hm}^2$  area of each  
237 forest type. LAI (Leaf area index) was measured using a LAI-2200 plant canopy  
238 analyzer with 90° view caps (Li-Cor Inc., USA). 10 observation points (distance of  
239 about 10 m) were selected in the 1  $\text{hm}^2$  area of each forest type with 5 replications.  
240 Growth indicators of the selected trees have been recorded: tree height (m), diameter at  
241 breast height (DBH, cm), and crown area (CA,  $\text{m}^2$ ). Tree height was measured using a  
242 laser range finder. A tape measure was used to measure the diameter of trees at a height  
243 of 1.3 m, namely DBH. CA: the laser rangefinder was used to measure the maximum  
244 diameter at the edge of the canopy, with multiple measurements at different points to  
245 ensure accuracy.



246 The differences in throughfall and stemflow among different forests were assessed  
247 using analysis of variance (ANOVA), followed by a Tukey test for multiple  
248 comparisons between means. Mann-Kendall (MK) test was used to analyze the  
249 variation trend of annual rainfall. All statistical procedures were conducted with  $\alpha =$   
250 0.05 threshold for significance, in the IBM SPSS statistics 22.0 software (IBM Inc.).

251

## 252 **3 Results**

### 253 **3.1 Rainfall and temperature characteristics**

254 Based on the 22-year rainfall dataset from the Dinghushan area, annual gross  
255 rainfall ranged between 1370.0 and 2361.1 mm (Fig. 1). 78.0% of gross rainfall  
256 appeared in the wet season (April–September). The M-K test showed that rainfall was  
257 significantly decreasing trend from 2001–2007 ( $UF < 0, P < 0.05$ ), and shifted into a  
258 significantly increasing pattern from 2012–2022 ( $UF > 0, P < 0.05$ ). Moreover, 2008  
259 and 2011 (the intersection of UF and UB) were the mutation time steps of the rainfall  
260 trend ( $P < 0.05$ ). Anomalies were revealed in the temporal variability (coefficient of  
261 variation,  $CV$  of 16.6%) in annual rainfall (Fig. 1a). Anomalies varied at -426.4–476.8  
262 mm and -258.0–471.4 mm in the wet season and dry season, respectively. By  
263 comparison, the dry season experienced greater variation with  $CV$  of 40.4% than the  
264 wet season with a  $CV$  of 21.7%. Besides, annual rain days tended to decrease over time  
265 from 2012 to 2021 (Fig. 1b). Based on five rainfall classifications, it was shown among  
266 22 years that rainfall  $< 10$  mm accounts for about 68.5% of total rain days (2856), while  
267 rainfall  $> 50$  mm account for about 4.9%. Besides, annual temperature changed between  
268 21.8 °C and 23.3 °C over 22 years. The M-K test showed a statistically significant  
269 increase in temperature for 8 years out of 22 years ( $UF > 0, P < 0.05$ ). Moreover, 2005  
270 and 2013–2014 were the mutation time steps of the temperature trend ( $P < 0.05$ ).

271

### 272 **3.2 Variability of throughfall**

273 Rainfall redistribution (throughfall and stemflow) among the three forests all  
274 experienced differing magnitudes for 22 years (Fig. 2). Annual throughfall was  
275 concentrated between 954.2 mm and 2192.6 mm. The M-K test showed that throughfall  
276 was in a significantly decreasing trend at first ( $UF < 0, P < 0.05$ ) and then shifted into  
277 a significant increase ( $UF > 0, P < 0.05$ ) from 2001–2022, similar to the trend of open  
278 rainfall. Differently, a mutation time step of throughfall occurred in 2008, 2011 and

279 2021 in the broadleaf forest, 2008 and 2011 in the mixed forest, 2006, 2008, 2011, and  
280 2021 in the pine forest ( $P < 0.05$ ). The throughfall ratio varied significantly both at  
281 event and interannual scales (Fig. 3a, b and c). The median annual throughfall ratio in  
282 the broadleaf forest varied between 60% and 120% with a  $CV$  of 16.4% from 2001–  
283 2022. The median throughfall ratio in the mixed pine and broadleaf forest varied  
284 between 80% and 110% with a  $CV$  of 9.7%. The median throughfall ratio in the pine  
285 forest varied between 59% and 110% with a  $CV$  of 11.8%. Therefore, the throughfall  
286 ratio was characterized by a low variability over an annual-time scale ( $CV < 20\%$ ).  
287 Besides, some differences in throughfall ratio were found among the three forest types  
288 based on rainfall classifications (Fig. 3d). For rainfall events  $<10$  mm, the throughfall  
289 ratio range in the broadleaf forest was 30%–70%, while in the other two forest types, it  
290 was 15%–85%. The mean value of the throughfall ratio was small in the broadleaf forest  
291 (53.9%), though no significant differences among the three forests ( $P > 0.05$ ) were  
292 detected. For rainfall events  $<50$  mm, no significant difference in throughfall ratio  
293 among the three forest types was found ( $P > 0.05$ ). However, the median values of the  
294 throughfall ratio in the pine forest (90.0%) and the mixed forest (89.4%) were both  
295 significantly larger than that in the broadleaf forest (83.7%) for rainfall events  $>50$  mm.  
296  $CV$  values of throughfall based on all the rainfall event classifications were drawn  
297 in the Fig. 4a. Results showed that the median  $CV$  of throughfall in the pine forest  
298 (15.2%) was lower than that for the broadleaf forest (21.7%) and for the mixed forest  
299 (26.3%) for rainfall events  $<10$  mm. For rainfall events  $>10$  mm, small differences in  
300 median  $CV$  among the three forest types were shown. Meanwhile,  $CV$  values decreased  
301 with the increasing rainfall events, eventually falling to 3.5%–4.3%. Besides,  $CV$  values  
302 of throughfall based on the interannual scale were drawn in the Fig. 5a, b and c. Annual  
303  $CV$  values among different forest types showed different fluctuations over time. The  
304 medians of  $CV$  in annual, wet and dry seasons presented different orders in different  
305 years. According to linear fitting, significant negative correlations were found in the  
306 median of  $CV_{TF}$  in the mixed forest over time ( $r = 0.63$ ,  $P < 0.01$ ). In addition, the fitted  
307 result of in total 740 rainfall events in 22 years showed that  $CV$  values of throughfall  
308 significantly decreased with increasing gross rainfall (Fig. S2).

309

### 310 **3.3 Variability of stemflow**

311 Annual stemflow was concentrated between 9.0 and 119.7 mm over 22 years (Fig.  
312 2). More stemflow was collected in the broadleaf forest and mixed forest than in the

313 pine forest. The M-K test showed that stemflow of both broadleaf forest and mixed  
314 forest was decreasing at first ( $UF < 0$ ,  $P < 0.05$ ) and then shifted into an increase ( $UF >$   
315  $0$ ,  $P < 0.05$ ), different from the continuously increasing trend of pine forest ( $UF > 0$ ).  
316 The mutation time steps of stemflow occurred in 2008 in the broadleaf forest, 2011 in  
317 the mixed forest, 2006, 2012 and 2015 in the pine forest ( $P < 0.05$ ). Stemflow ratio  
318 changed significantly both at the event and interannual scales (Fig. 3a, b and c). For 22  
319 years, the median annual stemflow ratio in the broadleaf forest varied between 1.3%  
320 and 5.4% with a  $CV$  of 56.2%. The stemflow ratio of mixed forest varied between 1.5%  
321 and 4.4% with a  $CV$  of 38.6%. In the pine forest, it varied between 0.3% and 1% with  
322 a  $CV$  of 50.9%. This indicated that the stemflow ratio was characterized by an extremely  
323 high variability over time. Similar to the seasonal throughfall ratio, the medians of  
324 stemflow ratios in annual, wet and dry seasons presented different orders in different  
325 years. Besides, the stemflow ratio significantly changed among tree species and rainfall  
326 classifications (Fig. 3e). By comparison, the stemflow ratios of the SF1 and SF2 trees  
327 in the broadleaf forest were both higher in all the tree species for the rainfall events  $< 50$   
328 mm. However, for strong events ( $> 50$  mm), the stemflow ratio of the SF5 tree in the  
329 mixed forest was highest for all tree species, followed by the trees in the broadleaf forest.  
330 For all the rainfall events, the stemflow ratio of SF7 in the mixed forest and SF8 in the  
331 pine forest were both lower than that for other tree species.

332  $CV$  values of stemflow based on rainfall event classifications were drawn in Fig.  
333 4b. By comparison, stemflow varied more than throughfall across all rainfall events,  
334 with  $CV_{SF}$  values of 25%–130%. Median  $CV$  of stemflow in the pine forest was always  
335 lower (45%–68%) than that for the other two forest types (56%–120%).  $CV$  values of  
336 stemflow based on an interannual scale changed over time among different forest types  
337 (Fig. 5d, e and f). The medians of  $CV_{SF}$  in annual, wet and dry seasons presented  
338 different orders in different years. By comparison,  $CV_{SF}$  was always greater than  $CV_{TF}$ ,  
339 and the interannual fluctuation of  $CV_{SF}$  was also stronger than  $CV_{TF}$ . According to linear  
340 fitting, significant negative correlations were found in the median of  $CV_{SF}$  in the  
341 broadleaf forest over time ( $r = 0.73$ ,  $P < 0.001$ ). In addition, the fitted result of in total  
342 740 rainfall events in 22 years showed that  $CV$  values of stemflow both significantly  
343 decreased with increasing gross rainfall (Fig. S2).

344

### 345 **3.4 Rainwater chemistry**

346 Rainwater (open rainfall, throughfall and stemflow) chemical properties (TN, TP  
347 and  $K^+$  concentration) were measured in the three forest types, respectively. All of TN,  
348 TP and  $K^+$  values are presented in the order stemflow > throughfall > open rainfall (Fig.  
349 6a, b and c). However, changes of TN, TP and  $K^+$  were different for the three forest  
350 types in 2000, 2010, and 2022. For instance, in 2000 and 2010, TN values of throughfall  
351 and stemflow decreased for both from pine forest to mixed forest to broadleaf forest,  
352 while no such result could be confirmed in 2022. Similarly, TP values of throughfall in  
353 the broadleaf forest were 1.3 times higher than in the pine forest in 2022, while TP  
354 values in the pine forest were 6.8 times higher than that in the broadleaf forest in 2000.  
355  $K^+$  values of stemflow in 2010 ( $6.76 \text{ mg L}^{-1}$ ) and 2022 ( $6.22 \text{ mg L}^{-1}$ ) were higher for  
356 the broadleaf forest than for the pine forest ( $3.76 \text{ mg L}^{-1}$  and  $2.46 \text{ mg L}^{-1}$ ), which was  
357 different from that in 2022.

358 TN, TP and  $K^+$  fluxes of stemflow were  $< 10 \text{ kg ha}^{-1} \text{ a}^{-1}$ ,  $0.2 \text{ kg ha}^{-1} \text{ a}^{-1}$ ,  $6 \text{ kg ha}^{-1}$   
359  $\text{a}^{-1}$ , respectively, and all lower than those of throughfall and open rainfall (Fig. 7d, e and  
360 f). In 2000, 2010, and 2022, TN fluxes ( $39.4\text{--}87.4 \text{ kg ha}^{-1} \text{ a}^{-1}$ ) were 1.2–1.8 times higher  
361 than that of open rainfall, 3.3–28.0 times higher than that of stemflow. TP fluxes ( $1.1\text{--}$   
362  $2.7 \text{ kg ha}^{-1} \text{ a}^{-1}$ ) were 1.0–2.3 times higher than that of open rainfall, 8.7–31.4 times  
363 higher than that of stemflow.  $K^+$  flux ( $21.5\text{--}59.2 \text{ kg ha}^{-1} \text{ a}^{-1}$ ) was 2.2–8.1 times higher  
364 than that of open rainfall, 2.2–26.8 times greater than that of stemflow. In addition, TN,  
365 TP and  $K^+$  fluxes of stemflow increased with succession from primary to climax,  
366 namely pine forest < mixed forest < broadleaf forest. Different from this, differences in  
367 chemical fluxes of throughfall were not found among different forests, nor among  
368 different periods.

369 Moreover, monthly chemical concentrations in rainfall, throughfall and stemflow  
370 showed distinct changes (Fig. 7). Monthly TN, TP and  $K^+$  concentrations of rainfall  
371 were always lower than those of stemflow for all trees. Monthly TN, TP and  $K^+$  of  
372 stemflow in the dry season were generally higher than in the wet season. High monthly  
373 TN concentrations of stemflow with SF6 of mixed forest and SF8 of pine forest were  
374 found, especially in the dry season with maximum TN concentrations of  $27.59 \text{ mg L}^{-1}$   
375 at SF6 and  $19.94 \text{ mg L}^{-1}$  at SF8, respectively. Differently, a high monthly  $K^+$   
376 concentration of stemflow at SF4 in broadleaf forest was found, with a maximum  $K^+$   
377 concentration of  $25.17 \text{ mg L}^{-1}$  in the dry season.

378

## 379 **4 Discussion**

### 380 **4.1 Open rainfall partitioned to throughfall and stemflow**

381 Studies in forests have confirmed that throughfall volume increased with  
382 increasing gross rainfall at the event scale, accounting for 60%–80% of gross rainfall  
383 (Ji et al., 2023; André et al., 2011; Carlyle-Moses, 2004). Throughfall ratio changed  
384 over time and showed different fluctuations among different forests (Fig. 3). During  
385 light rainfall events with rainfall amounts <10 mm, a low proportion of raindrops would  
386 reach the ground as throughfall, as the tree canopy intercepts almost all the incoming  
387 raindrops. Specifically, high canopy coverage in broadleaf forests can reinforce  
388 raindrop intercept (Brasil et al., 2018; Ponette-González et al., 2010), consequently  
389 generating a lower throughfall ratio than those in the mixed forest and pine forest (Fig.  
390 3). During moderate rainfall events (10–50 mm), given that the intercept effect of the  
391 wetting tree canopy was weakened (Shinohara et al., 2015), throughfall ratio was in a  
392 high and steady state. As the gross rainfall increases further (>50 mm), significant  
393 differences of throughfall ratio were found among the three forests. The throughfall  
394 ratio was significantly lower in the broadleaf forest than those in the other two forests.  
395 Likewise, such differences due to the rainfall event class also appeared in other forest  
396 studies with stands formed by beech, pine in monocultures and mixed pine-beech  
397 (Blume et al., 2022). Influenced by forest stand characteristics, throughfall therefore  
398 indicated different forest water budgets.

399 Stemflow of forests was variably controlled by tree species, on average accounting  
400 for about <10% of gross rainfall, and partly even lower (<1%) (Sun et al., 2018; André  
401 et al., 2008; Crockford and Richardson, 1990). In our study site, the lowest stemflow  
402 (<1%) was collected in the pine forest, though weakly increasing with rainfall  
403 classifications (Fig. 3). Stemflow ratio in the broadleaf forest was maintained at 5%–  
404 10% without the effect of rainfall amount seemingly. In detail, stemflow ratio of pine  
405 forest (SF8) was significantly lower than those of broadleaf forest (SF1~4). In the  
406 mixed forest, broad-leaved trees (SF5 and SF6) have larger stemflow than pine trees  
407 (SF7). However, for some rainfall events, a particularly low proportion of stemflow in  
408 the broadleaf forest and an extraordinarily high proportion in the pine forest were  
409 caught. This implied the key role of rainfall conditions (e.g., intensity, duration) and  
410 tree species with tree traits (e.g., branch angle), consistent with reported studies e.g., in

411 an evergreen forest (Chen et al., 2019; Bruijnzeel et al., 2011) and pine forest (Pinos et  
412 al., 2021; Crockford and Richardson, 1990). Moreover, ANOVA showed significant  
413 differences in stemflow ratio among tree species and rainfall classifications ( $P < 0.001$ )  
414 (Table 1). This indicated that rainfall and tree species simultaneously affect stemflow.  
415 Branch inclination angle, canopy cover, tree height and DBH of tree species proved to  
416 be key factors in stemflow yield (Levia et al., 2015).

417 Throughfall and stemflow were generally enriched in chemical concentration  
418 compared with open rainfall due to leachable canopy/stem ion pools (Jiang et al., 2021;  
419 Van Stan et al., 2017; Zimmermann et al., 2007). In our study, the concentration of  $K^+$   
420 in stemflow was 16 times higher than that in open rainfall and in throughfall reached  
421 up to 11 times higher than open rainfall (Fig. 6). Similar results were also found in  
422 forestry plantations (*Acacia mangium* and *Dimocarpus longan*) of South China (Shen  
423 et al., 2013), or in Oriental beech (*Fagus orientalis* Lipsky) trees in Northern Iran  
424 (Moslehi et al., 2019), indicating strong  $K^+$  leaching from the canopy. Even so,  
425 throughfall was generally characterized by high fluxes compared to open rainfall  
426 followed by stemflow, it thus is the largest contributor to wet deposition. Meanwhile,  
427 the TN flux of throughfall was greatest in the pine forest in 2010, the TP flux of  
428 throughfall was greatest in the broadleaf forest in 2000, and the  $K^+$  flux of throughfall  
429 was greatest in the mixed forest in 2010. It should be noted that the differences in  
430 rainwater chemistry shifted over time among the three forests. Accordingly, throughfall  
431 and stemflow via the canopy and stem to the soil are a significant contributor, and their  
432 long-term effect on ecosystems needs more scientific attention (Fan et al., 2021). After  
433 all, atmospheric wet deposition provides important nutrient amounts for ecosystems,  
434 but also imposes a considerable burden on the ecosystems in general. For instance, N  
435 enrichment and P limitation have proven to have different effects on soil carbon  
436 sequestration, microbial community composition and forest productivity, especially in  
437 tropical and subtropical forest ecosystems with highly weathered soils (Zheng et al.,  
438 2022; Li et al., 2016; Huang et al., 2012). Besides, throughfall and stemflow was mainly  
439 characterized by low chemical concentrations in the wet season and high concentrations  
440 in the dry season. Primary reasons for seasonal rainwater chemistry may be attributable  
441 to moisture source associated with frontal weather systems and gradually depleting  
442 effect with increasing rainfall amount (Dunkerley, 2014; Germer et al., 2007). The  
443 present study in subtropical forests and previous studies in tropical forests and European  
444 temperate forests all exhibited variable rainwater chemistry in throughfall and stemflow,

445 both spatially and temporally (Zimmermann et al., 2007; Staelens et al., 2006; Seiler  
446 and Matzner, 1995). The chemical concentration of rainfall redistribution was also  
447 affected profoundly by canopy and stem parameters of tree species (Tonello et al.,  
448 2021b; Chen et al., 2019). In our study, some differences in TN, TP and  $K^+$  were also  
449 found among SF1~SF8 due to tree-species-specific effects (Legout et al., 2016; De  
450 Schrijver et al., 2007).

451

## 452 **4.2 Long-term changes in rainfall in forests**

453 Rainfall regimes induce divergent spatially hydrological changes (Wu et al., 2024).  
454 Likewise, our study found that the throughfall of forests experienced a decrease  
455 followed by an increase from 2001–2022, similar to the trend of open rainfall, and  
456 stemflow showed characteristic trends in different forests especially in the pine forest  
457 (Fig. 1). This suggested that the complexity of forest structure and rainfall amount and  
458 their change exacerbated the spatio-temporal variability of throughfall and stemflow.  
459 Firstly, interannual variability of forest structure (e.g., canopy coverage, leaf area index)  
460 and tree parameters (e.g., height, DBH, and CA) made throughfall and stemflow  
461 distribution uncertain (Yue et al., 2021). From 2001 to 2022, changes in forest structure  
462 were confirmed in all three forests, such as changes in plant density, canopy coverage  
463 and LAI (Fig. 8). Throughfall ratio and stemflow ratio in the succession forest systems  
464 all varied over time accordingly. Similarly, driven by forest structure (e.g., tree density,  
465 species dominance), a six-year dataset from the Brazilian Atlantic Forest showed that  
466 the spatial variability of throughfall over time was less stable (Rodrigues et al., 2022).  
467 Besides, the variation of stemflow ( $CV_{SF}$ ) was larger than that of throughfall ( $CV_{TF}$ )  
468 (Fig. 4), which probably was attributed to the differences of tree species in stemflow  
469 (Fig. 3). For a forest succession, a 17 years' study showed that the shift from  
470 monoculture Japanese red pine to mixture of red pine, evergreen oak and deciduous  
471 trees made stemflow significantly increasing (Iida et al., 2005). Likewise, for the forest  
472 succession in Dinghushan area, stemflow ratio in the broadleaf forest and mixed forest  
473 were both higher than that in the tree-monospecific pine forest. High plant density (tree  
474 and shrub) and LAI in broadleaf forest and mixed forest conduce to rainwater  
475 interception of multi-canopy trees through more leaves and angled branches, which  
476 potentially enhanced stemflow (Fig. 8). Indeed, some differences of rainfall  
477 redistribution appeared in multi-layered vegetative structure. An experiment on  
478 vegetation communities with a complex multi-layered structure found that interception

479 loss from shrubs was two times higher than from trees, and smaller trees generated  
480 stemflow more efficiently than the higher ones (Exler and Moore, 2022). Based on the  
481 22 years' data from the forest community survey in our study site, forest canopy  
482 parameters (e.g., coverage and LAI) of trees and shrubs showed variation over time  
483 from 2001 to 2022 (Fig. 8). In the broadleaf forest, plant density of trees and canopy  
484 coverage of shrubs showed a slight increment compared to the other two forest types,  
485 though LAI was decreasing. During this period, interannual throughfall ratio and  
486 stemflow ratio showed significant change over time (Fig. 3), implying the role of  
487 interannual variation of forest structure in the rainfall redistribution process.

488 Secondly, ongoing rainfall changes with different magnitudes favor the different  
489 levels of rainfall redistribution over time (Lian et al., 2022). At the event scale,  
490 throughfall and stemflow proportions of forests were both low with rainfall events <10  
491 mm. The variations of throughfall and stemflow were both larger for gross rainfall <10  
492 mm than events >10 mm. Rainfall threshold associated with the canopy interception  
493 capacity had an impact on throughfall and stemflow generation (Zabret et al., 2018;  
494 André et al., 2008; Durocher, 1990). After the raindrop capacity of the canopy reached  
495 its peak, throughfall and stemflow were documented to match the gross rainfall.  
496 Therefore, low proportions and high spatial variability appeared before the rainfall  
497 threshold, and after that, relatively high proportions and low variability until a stable  
498 level were observed in the three forests. Moreover, at the interannual scale, the rain days  
499 in different magnitudes presented fluctuation over 22 years (Fig. 1). This fluctuation of  
500 rain days and its magnitude distribution potentially regulated the long-term changes of  
501 open rainfall partitioned to interception loss, throughfall and stemflow. Consequently,  
502 throughfall and stemflow, influenced by the comprehensive effect of rainfall regimes  
503 and forest structures, presented spatiotemporal variability at different levels (Fig. 3–6).  
504 From a long-term perspective, changes in rainfall redistribution potentially make forest  
505 water and biogeochemistry budgets more complex. Further knowledge of the long-term  
506 accumulative effect of rainfall redistribution on forest water and chemistry (e.g., soil  
507 and plant) is needed in the future.

508 Throughfall and stemflow are part of rainfall and are key players in the water cycle  
509 process. Based on the connection of the water cycle to precipitation and temperature  
510 and under the background of climate change, the frequency of extreme events (heavy  
511 rainfall, droughts) needs to be anticipated in the effect on rainfall redistribution and  
512 solute transport within forests, which in turn may affect the water cycle and



513 biogeochemical cycles (Blume et al., 2022). In this study, it should be noted that the  
514 2008 rainfall data can be used as an example of an extreme event. In 2008, extreme  
515 weather events occurred in South China. Freezing events occurred in the dry season,  
516 and continuous heavy rain and typhoon events occurred in the wet season. Gross rainfall  
517 was larger than in other years, with an annual rainfall of 2361.1 mm (22-year average  
518 annual rainfall of 1848.6 mm) (Fig. 1). At the same time, a total of 26 throughfall events  
519 were collected in 2008. The throughfall and stemflow trend of different forests  
520 presented different degrees of disturbance under the background of mutation of open  
521 rainfall (Fig. 2). In this process, the driving effect of forest structure and rainfall on  
522 throughfall and stemflow mutation is synchronous. More data and modeling are needed  
523 to support the relevant study about the effect of climate change on rainfall redistribution  
524 in the future.

525

## 526 **5 Conclusions**

527 The current study investigated long-term changing characteristics of rainfall  
528 redistribution along a subtropical forest succession sequence with pine forest (PF),  
529 mixed pine and broadleaf forest (MF), and monsoon evergreen broadleaf forest (BF).  
530 Firstly, in the 740 measured rainfall events, the throughfall ratio changed from BF <  
531 MF < PF, and the stemflow ratio changed from BF > MF > PF. The variation of  
532 stemflow was higher ( $CV > 50\%$ ) than that of throughfall ( $CV < 25\%$ ). Secondly,  
533 throughfall and stemflow of the investigated forests experienced a decrease followed  
534 by an increase from 2001–2022 (except stemflow of the pine forest), similar to the trend  
535 of open rainfall. Driven by rainfall and forest factors, the interannual variability of both  
536 throughfall and stemflow in the broadleaf forest was higher than those in the mixed  
537 forest and pine forest, which was different from that of annual open rainfall.

538 For rainwater chemistry, differences in the element fluxes in throughfall and  
539 stemflow among the three forest types were confirmed based on data from 2001, 2010,  
540 and 2022. On average, TN and TP fluxes of throughfall developed from BF < MF < PF,  
541 while  $K^+$  flux of throughfall changed from BF > MF > PF. Over time, rainwater  
542 chemical concentrations were lower in the wet season than in the dry season. Given the  
543 smaller proportion of open rainfall, stemflow chemical fluxes varied less among forest  
544 types and over time, though tree species exactly represented the differences in stemflow  
545 chemistry. Nevertheless, its funnel effect on soil and plants over time still deserves more  
546 scientific attention in the future.

547 The above results indicate that the water volume and chemistry of rainfall during  
548 redistribution processes under forests represent not the same trend as open rainfall over  
549 time, and throughfall and stemflow depend on the effect of rainfall and forest factors.  
550 This study thus provides insight into the rainfall redistribution process by linking the  
551 long-term change of rainfall patterns with a subtropical forest succession sequence.

552

553

554 *Code and data availability.* The data used to derive to the conclusions of the present  
555 study are freely accessible. All the data were obtained from the CNERN dataset  
556 (<http://dhf.cern.ac.cn/meta/metaData>).

557

558 *Author contributions.* WJZ: conceptualization, investigation, data analysis, writing,  
559 visualization. TS and SS: reviewing, supervision. QMZ and GWC: resources, data  
560 curation, LHW: reviewing, JXL and XX: reviewing, funding acquisition, supervision

561

562 *Competing interests.* The authors declare that they have no conflict of interest.

563

564 *Disclaimer.* Publisher's note: Copernicus Publications remains neutral with regard to  
565 jurisdictional claims made in the text, published maps, institutional affiliations, or any  
566 other geographical representation in this paper. While Copernicus Publications makes  
567 every effort to include appropriate place names, the final responsibility lies with the  
568 authors.

569

570 *Acknowledgements.* Wanjun Zhang would like to acknowledge the financial support  
571 from the CSC Fellowship.

572

573 *Financial support.* This research has been supported by The Key-Area Research and  
574 Development Program of Guangdong Province (Grant No. 2022B1111230001), the  
575 National Natural Science Foundation of China (Grant Nos. 42207158 and 32101342)  
576 and the China Postdoctoral Science Foundation (Grant Nos. 2021M703259, 2021  
577 M703260, 2021M693220).

578

579 *Review statement.* This paper was edited by Loes van Schaik and reviewed by two  
580 anonymous referees.

581

582

583 **References**

584 André, F., Jonard, M., Jonard, F., and Ponette, Q.: Spatial and temporal patterns of throughfall volume in  
585 a deciduous mixed-species stand, *J. Hydrol.*, 400(1–2), 244–254,  
586 <https://doi.org/10.1016/j.jhydrol.2011.01.037>, 2011.

587 André, F., Jonard, M., and Ponette, Q.: Influence of species and rain event characteristics on stemflow  
588 volume in a temperate mixed oak–beech stand, *Hydrol. Process.*, 22(22), 4455–4466,  
589 <https://doi.org/10.1002/hyp.7048>, 2008.

590 Blume, T., Schneider, L., and Güntner, A.: Comparative analysis of throughfall observations in six  
591 different forest stands: Influence of seasons, rainfall-and stand characteristics, *Hydrol. Process.*,  
592 36(3), e14461, <https://doi.org/10.1002/hyp.14461>, 2022.

593 Borghetti, M., Gentilesca, T., Leonardi, S., Van Noije, T., and Rita, A.: Long-term temporal relationships  
594 between environmental conditions and xylem functional traits: a meta-analysis across a range of  
595 woody species along climatic and nitrogen deposition gradients, *Tree Physiol.*, 37(1), 4–17,  
596 <https://doi.org/10.1093/treephys/tpw087>, 2017.

597 Brasil, J.B., Andrade, E.M.d., Palácio, H.A.d.Q., Medeiros, P.H.A., and Santos, J.C.N.d.: Characteristics  
598 of precipitation and the process of interception in a seasonally dry tropical forest, *J. Hydrol-Reg.*  
599 *Stud.*, 19, 307–317, <https://doi.org/10.1016/j.ejrh.2018.10.006>, 2018.

600 Brauman, K.A., Freyberg, D.L., and Daily, G.C.: Forest structure influences on rainfall partitioning and  
601 cloud interception: A comparison of native forest sites in Kona, Hawai’I, *Agric. For. Meteorol.*,  
602 150(2), 265–275, <https://doi.org/10.1016/j.agrformet.2009.11.011>, 2010.

603 Bruijnzeel, L.A., Mulligan, M., and Scatena, F.N.: Hydrometeorology of tropical montane cloud forests:  
604 emerging patterns, *Hydrol. Process.*, 25(3), 465–498, <https://doi.org/10.1002/hyp.7974>, 2011.

605 Carlyle-Moses, D.E., Laureano, J.F., and Price, A.G.: Throughfall and throughfall spatial variability in  
606 Madrean oak forest communities of northeastern Mexico, *J. Hydrol.*, 297(1–4), 124–135,  
607 <https://doi.org/10.1016/j.jhydrol.2004.04.007>, 2004.

608 Chen, S., Cao, R., Yoshitake, S., and Ohtsuka, T.: Stemflow hydrology and DOM flux in relation to tree  
609 size and rainfall event characteristics, *Agric. For. Meteorol.*, 279, 107753,  
610 <https://doi.org/10.1016/j.agrformet.2019.107753>, 2019.

611 Crockford, R.H., and Richardson, D.P.: Partitioning of rainfall in a eucalypt forest and pine plantation in  
612 southeastern Australia: II Stemflow and factors affecting stemflow in a dry sclerophyll eucalypt  
613 forest and a *Pinus radiata* plantation, *Hydrol. Process.*, 4(2), 145–155,  
614 <https://doi.org/10.1002/hyp.3360040205>, 1990.

615 De Schrijver, A., Geudens, G., Augusto, L., Staelens, J., Mertens, J., Wuyts, K., Gielis, L., and Verheyen,  
616 K.: The effect of forest type on throughfall deposition and seepage flux: a review, *Oecologia*, 153,  
617 663–674, <https://doi.org/10.1007/s00442-007-0776-1>, 2007.

618 Dunkerley, D.: Stemflow on the woody parts of plants: dependence on rainfall intensity and event profile  
619 from laboratory simulations, *Hydrol. Process.*, 28(22), 5469–5482,  
620 <https://doi.org/10.1002/hyp.10050>, 2014.

621 Durocher, M.G.: Monitoring spatial variability of forest interception, *Hydrol. Process.*, 4(3), 215–229,  
622 <https://doi.org/10.1002/hyp.3360040303>, 1990.

623 Exler, J.L., and Moore, R.D.: Quantifying throughfall, stemflow and interception loss in five vegetation  
624 communities in a maritime raised bog, *Agric. For. Meteorol.*, 327, 109202,  
625 <https://doi.org/10.1016/j.agrformet.2022.109202>, 2022.

626 Fan, Y.X., Lu, S.X., He, M., Yang, L.M., Hu, W.F., Yang, Z.J., Liu, X.F., Hui, D.F., Guo, J.F., and Yang,  
627 Y.S.: Long-term throughfall exclusion decreases soil organic phosphorus associated with reduced  
628 plant roots and soil microbial biomass in a subtropical forest, *Geoderma*, 404, 115309,  
629 <https://doi.org/10.1016/j.geoderma.2021.115309>, 2021.

630 Germer, S., Elsenbeer, H., and Moraes, J.M.: Throughfall and temporal trends of rainfall redistribution  
631 in an open tropical rainforest, south-western Amazonia (Rondônia, Brazil), *Hydrol. Earth Syst. Sci.*,  
632 10(3), 383–393, <https://doi.org/10.5194/hess-10-383-2006>, 2006.

633 Germer, S., Neill, C., Krusche, A.V., Neto, S.C.G., and Elsenbeer, H.: Seasonal and within-event  
634 dynamics of rainfall and throughfall chemistry in an open tropical rainforest in Rondônia, Brazil,  
635 *Biogeochemistry*, 86, 155–174, <https://doi.org/10.1007/s10533-007-9152-9>, 2007.

636 Germer, S., Werther, L., and Elsenbeer, H.: Have we underestimated stemflow? Lessons from an open  
637 tropical rainforest, *J. Hydrol.*, 395(3-4), 169–179, <https://doi.org/10.1016/j.jhydrol.2010.10.022>,  
638 2010.

639 Goebes, P., Bruelheide, H., Härdtle, W., Kröber, W., Kühn, P., Li, Y., Seitz, S., von Oheimb, G., and  
640 Scholten, T.: Species-specific effects on throughfall kinetic energy in subtropical forest plantations  
641 are related to leaf traits and tree architecture, *PLoS one*, 10(6), e0128084,  
642 <https://doi.org/10.1371/journal.pone.0128084>, 2015.

643 Grunicke, S., Queck, R., and Bernhofer, C.: Long-term investigation of forest canopy rainfall interception  
644 for a spruce stand, *Agric. For. Meteorol.*, 292, 108125,  
645 <https://doi.org/10.1016/j.agrformet.2020.108125>, 2020.

646 Grossiord, C., Sevanto, S., Dawson, T. E., Adams, H.D., Collins, A.D., Dickman, L.T., Newman B.D.,  
647 Stockton, E.A., and McDowell, N.G.: Warming combined with more extreme precipitation regimes  
648 modifies the water sources used by trees, *New Phytol.*, 213(2), 584–596,  
649 <https://doi.org/10.1111/nph.14192>, 2017.

650 Huang, W.J., Zhou, G.Y., and Liu, J.X.: Nitrogen and phosphorus status and their influence on  
651 aboveground production under increasing nitrogen deposition in three successional forests, *Acta*  
652 *Oecologica*, 44, 20–27, <https://doi.org/10.1016/j.actao.2011.06.005>, 2012.

653 Iida, S.I., Tanaka, T., and Sugita, M.: Change of interception process due to the succession from Japanese  
654 red pine to evergreen oak, *J. Hydrol.*, 315(1–4), 154–166,  
655 <https://doi.org/10.1016/j.jhydrol.2005.03.024>, 2005.

656 Jackson, N.A.: Measured and modelled rainfall interception loss from an agroforestry system in Kenya,  
657 *Agric. For. Meteorol.*, 100, 323–336, [https://doi.org/10.1016/S0168-1923\(99\)00145-8](https://doi.org/10.1016/S0168-1923(99)00145-8), 2000.

658 Ji, S.Y., Omar, S.I., Zhang, S.B., Wang, T.F., Chen, C.F., and Zhang, W.J.: Comprehensive evaluation of  
659 throughfall erosion in the banana plantation, *Earth Surf. Proc. Land.*, 47(12), 2941–2949,  
660 <https://doi.org/10.1002/esp.5435>, 2022.

661 Jiang, Z.Y., Zhi, Q.Y., Van Stan, J.T., Zhang, S.Y., Xiao, Y.H., Chen, X.Y., and Wu, H.W.: Rainfall  
662 partitioning and associated chemical alteration in three subtropical urban tree species, *J. Hydrol.*,  
663 603, 127109, <https://doi.org/10.1016/j.jhydrol.2021.127109>, 2021.

664 Junior, J.J., Mello, C.R., Owens, P.R., Mello, J.M., Curi, N., and Alves, G.J.: Time-stability of soil water  
665 content (SWC) in an Atlantic Forest-Latosol site, *Geoderma*, 288, 64–78,  
666 <https://doi.org/10.1016/j.geoderma.2016.10.034>, 2017.

667 Keim, R.F., Tromp-van Meerveld, H.J., and McDonnell, J.J.: A virtual experiment on the effects of  
668 evaporation and intensity smoothing by canopy interception on subsurface stormflow generation, *J.*  
669 *Hydrol.*, 327(3–4), 352–364, <https://doi.org/10.1016/j.jhydrol.2005.11.024>, 2006.

670 Klos, P.Z., Chain-Guadarrama, A., Link, T.E., Finegan, B., Vierling, L.A., and Chazdon, R.: Throughfall  
671 heterogeneity in tropical forested landscapes as a focal mechanism for deep percolation, *J. Hydrol.*,  
672 519, 2180–2188, <https://doi.org/10.1016/j.jhydrol.2014.10.004>, 2014.

673 Kottek, M., Grieser, J., Beck, C., Rudolf, B., and Rubel, F.: World map of the Köppen-Geiger climate  
674 classification updated, *Meteorol. Z.*, 15(3), 259–263, <https://doi.org/10.1127/0941-2948/2006/0130>,  
675 2006.

676 Lacombe, G., Valentin, C., Sounyafong, P., De Rouw, A., Soulileuth, B., Silvera, N., Pierret, A.,  
677 Sengtaheuanghong, O., and Ribolzi, O.: Linking crop structure, throughfall, soil surface conditions,  
678 runoff and soil detachment: 10 land uses analyzed in Northern Laos, *Sci. Total Environ.*, 616, 1330–  
679 1338, <https://doi.org/10.1016/j.scitotenv.2017.10.185>, 2018.

680 Legout, A., van Der Heijden, G., Jaffrain, J., Boudot, J. P., and Ranger, J.: Tree species effects on solution  
681 chemistry and major element fluxes: A case study in the Morvan (Breuil, France), *Forest Ecol.*  
682 *Manag.*, 378, 244–258, <https://doi.org/10.1016/j.foreco.2016.07.003>, 2016.

683 Leuzinger, S., and Körner, C.: Rainfall distribution is the main driver of runoff under future CO<sub>2</sub>-  
684 concentration in a temperate deciduous forest, *Global Change Biol.*, 16(1), 246–254,  
685 <https://doi.org/10.1111/j.1365-2486.2009.01937.x>, 2010.

686 Levia, D. F., Nanko, K., Amasaki, H., Giambelluca, T. W., Hotta, N., Iida, S. I., Mudd, R.G., Nullet, M.A.,  
687 Sakai, N., Shinori, Y., Sun X.C., Suzuki, M., Tanaka, N., Tantasirin, C., and Yamada, K.: Throughfall  
688 partitioning by trees, *Hydrol. Process.*, 33(12), 1698–1708, <https://doi.org/10.1002/hyp.13432>, 2019.

689 Levia, D.F., and Germer, S.: A review of stemflow generation dynamics and stemflow-environment  
690 interactions in forests and shrublands, *Rev. Geophys.*, 53(3), 673–714,  
691 <https://doi.org/10.1002/2015RG000479>, 2015.

692 Levia Jr, D.F., and Frost, E.E.: Variability of throughfall volume and solute inputs in wooded ecosystems,  
693 *Prog. Phys. Geog.*, 30(5), 605–632, <https://doi.org/10.1177/0309133306071145>, 2006.

694 Li, Y., Niu, S.L, and Yu, G.R.: Aggravated phosphorus limitation on biomass production under increasing  
695 nitrogen loading: a meta-analysis, *Global Change Biol.*, 22(2), 934–943,  
696 <https://doi.org/10.1111/gcb.13125>, 2016.

697 Lian, X., Zhao, W.L., and Gentine, P., 2022. Recent global decline in rainfall interception loss due to  
698 altered rainfall regimes. *Nat. Commun.* 13(1), 7642. <https://doi.org/10.1038/s41467-022-35414-y>

699 Liu, J.Q., Liu, W.J., Li, W.X., and Zeng, H.H.: How does a rubber plantation affect the spatial variability  
700 and temporal stability of throughfall?, *Hydrol. Res.*, 50(1), 60–74,

701 <https://doi.org/10.2166/nh.2018.028>, 2019.

702 Livesley, S.J., Baudinette, B., and Glover, D.: Rainfall interception and stem flow by eucalypt street trees  
703 – The impacts of canopy density and bark type, *Urban For. Urban Gree.*, 13(1), 192–197,  
704 <https://doi.org/10.1016/j.ufug.2013.09.001>, 2014.

705 Llorens, P., and Domingo, F.: Rainfall partitioning by vegetation under Mediterranean conditions. A  
706 review of studies in Europe, *J. Hydrol.*, 335(1–2), 37–54,  
707 <https://doi.org/10.1016/j.jhydrol.2006.10.032>, 2007.

708 Llorens, P., Latron, J., Carlyle-Moses, D.E., Nätthe, K., Chang, J.L., Nanko, K., Lida, S., and Levia, D.F.:  
709 Stemflow infiltration areas into forest soils around American beech (*Fagus grandifolia* Ehrh.) trees,  
710 *Ecohydrology*, 15(2), e2369, <https://doi.org/10.1002/eco.2369>, 2022.

711 Loustau, D., Berbigier, P., and Granier, A.: Interception loss, throughfall and stemflow in a maritime pine  
712 stand. II. An application of Gash's analytical model of interception, *J. Hydrol.*, 138(3–4), 469–485,  
713 [https://doi.org/10.1016/0022-1694\(92\)90131-E](https://doi.org/10.1016/0022-1694(92)90131-E), 1992.

714 Marin, C.T., Bouten, W., and Sevink, J.: Gross rainfall and its partitioning into throughfall, stemflow and  
715 evaporation of intercepted water in four forest ecosystems in western Amazonia, *J. Hydrol.*, 237(1–  
716 2), 40–57, [https://doi.org/10.1016/S0022-1694\(00\)00301-2](https://doi.org/10.1016/S0022-1694(00)00301-2), 2000.

717 Moslehi, M., Habashi, H., Khormali, F., Ahmadi, A., Brunner, I., and Zimmermann, S.: Base cation  
718 dynamics in rainfall, throughfall, litterflow and soil solution under Oriental beech (*Fagus orientalis*  
719 Lipsky) trees in northern Iran, *Ann. Forest Sci.*, 76(2), 1–12, <https://doi.org/10.1007/s13595-019-0837-8>, 2019.

721 Muzyło, A., Llorens, P., and Domingo, F.: Rainfall partitioning in a deciduous forest plot in leafed and  
722 leafless periods, *Ecohydrology*, 5(6), 759–767, <https://doi.org/10.1002/eco.266>, 2012.

723 Nanko, K., Hotta, N., and Suzuki, M.: Evaluating the influence of canopy species and meteorological  
724 factors on throughfall drop size distribution, *J. Hydrol.*, 329(3–4), 422–431,  
725 <https://doi.org/10.1016/j.jhydrol.2006.02.036>, 2006.

726 Niu, X.T., Fan, J., Du, M.G., Dai, Z.J., Luo, R.H., Yuan, H.Y., and Zhang, S.G.: Changes of Rainfall  
727 Partitioning and canopy interception modeling after progressive thinning in two shrub plantations  
728 on the Chinese Loess Plateau, *J. Hydrol.*, 619, 129299,  
729 <https://doi.org/10.1016/j.jhydrol.2023.129299>, 2023.

730 Pinos, J., Latron, J., Levia, D. F., and Llorens, P.: Drivers of the circumferential variation of stemflow  
731 inputs on the boles of *Pinus sylvestris* L. (Scots pine), *Ecohydrology*, 14(8), e2348,  
732 <https://doi.org/10.1002/eco.2348>, 2021.

733 Ponette-González, A.G., Weathers, K.C., and Curran, L.M.: Water inputs across a tropical montane  
734 landscape in Veracruz, Mexico: synergistic effects of land cover, rain and fog seasonality, and  
735 interannual precipitation variability, *Global Change Biol.*, 16(3), 946–963,  
736 <https://doi.org/10.1111/j.1365-2486.2009.01985.x>, 2010.

737 Price, A.G., Dunham, K., Carleton, T., and Band, L.: Variability of water fluxes through the black spruce  
738 (*Picea mariana*) canopy and feather moss (*Pleurozium schreberi*) carpet in the boreal forest of  
739 Northern Manitoba, *J. Hydrol.*, 196(1–4), 310–323, [https://doi.org/10.1016/S0022-1694\(96\)03233-7](https://doi.org/10.1016/S0022-1694(96)03233-7),  
740 1997.

741 Reynaert, S., De Boeck, H.J., Verbruggen, E., Verlinden, M., Flowers, N., and Nijs, I.: Risk of short-term  
742 biodiversity loss under more persistent precipitation regimes, *Global Change Biol.*, 27(8), 1614–  
743 1626, <https://doi.org/10.1111/gcb.15501>, 2021.

744 Rodrigues, A.F., Terra, M.C., Mantovani, V.A., Cordeiro, N.G., Ribeiro, J.P., Guo, L., Nehren, U., Mello,  
745 M.J., and Mello, C.R.: Throughfall spatial variability in a neotropical forest: Have we correctly  
746 accounted for time stability?, *J. Hydrol.*, 608, 127632,  
747 <https://doi.org/10.1016/j.jhydrol.2022.127632>, 2022.

748 Seiler, J., and Matzner, E.: Spatial variability of throughfall chemistry and selected soil properties as  
749 influenced by stem distance in a mature Norway spruce (*Picea abies*, Karst.) stand, *Plant Soil*, 176,  
750 139–147, <https://doi.org/10.1007/BF00017684>, 1995.

751 Shen, W.J., Ren, H.L., Jenerette, G.D., Hui, D.F., and Ren, H.: Atmospheric deposition and canopy  
752 exchange of anions and cations in two plantation forests under acid rain influence, *Atmos Environ.*,  
753 64, 242–250, <https://doi.org/10.1016/j.atmosenv.2012.10.015>, 2013.

754 Shinohara, Y., Levia, D.F., Komatsu, H., Nogata, M., and Otsuki, K.: Comparative modeling of the effects  
755 of intensive thinning on canopy interception loss in a Japanese cedar (*Cryptomeria japonica* D. Don)  
756 forest of western Japan, *Agric. For. Meteorol.*, 214–215, 148–156,  
757 <https://doi.org/10.1016/j.agrformet.2015.08.257>, 2015.

758 Siegert, C.M., and Levia, D.F.: Seasonal and meteorological effects on differential stemflow funneling  
759 ratios for two deciduous tree species, *J. Hydrol.*, 519, 446–454,  
760 <https://doi.org/10.1016/j.jhydrol.2014.07.038>, 2014.

761 Staelens, J., De Schrijver, A., and Verheyen, K.: Seasonal variation in throughfall and stemflow chemistry  
762 beneath a European beech (*Fagus sylvatica*) tree in relation to canopy phenology, *Can. J. Forest*  
763 *Res.*, 37(8), 1359–1372, <https://doi.org/10.1139/X07-003>, 2007.

764 Staelens, J., De Schrijver, A., Verheyen, K., and Verhoest, N.E.: Spatial variability and temporal stability  
765 of throughfall deposition under beech (*Fagus sylvatica* L.) in relationship to canopy structure,  
766 *Environ. Pollut.*, 142(2), 254–263, <https://doi.org/10.1016/j.envpol.2005.10.002>, 2006.

767 Su, L., Zhao, C.M., Xu, W.T., and Xie, Z.Q.: Hydrochemical fluxes in bulk precipitation, throughfall,  
768 and stemflow in a mixed evergreen and deciduous broadleaved forest, *Forests*, 10(6), 507,  
769 <https://doi.org/10.3390/f10060507>, 2019.

770 Sun, J.M., Yu, X.X., Wang, H.N., Jia, G.D., Zhao, Y., Tu, Z.H., Deng, W.P., Jia, J.B., and Chen, J.G.  
771 Effects of forest structure on hydrological processes in China, *J. Hydrol.*, 561, 187–199,  
772 <https://doi.org/10.1016/j.jhydrol.2018.04.003>, 2018.

773 Sun, S.Y., Liu, X.F., Lu, S.X., Cao, P.L., Hui, D.F., Chen, J., Guo, J.F., and Yang, Y.S.: Depth-dependent  
774 response of particulate and mineral-associated organic carbon to long-term throughfall reduction in  
775 a subtropical natural forest, *Catena*, 223, 106904, <https://doi.org/10.1016/j.catena.2022.106904>,  
776 2023.

777 Tonello, K.C., Rosa, A.G., Pereira, L.C., Matus, G.N., Guandique, M.E.G., and Navarrete, A.A.: Rainfall  
778 partitioning in the Cerrado and its influence on net rainfall nutrient fluxes, *Agric. For. Meteorol.*,  
779 303, 108372, <https://doi.org/10.1016/j.agrformet.2021.108372>, 2021a.

780 Tonello, K.C., Van Stan II, J.T., Rosa, A.G., Balbinot, L., Pereira, L.C., and Bramorski, J.: Stemflow

781 variability across tree stem and canopy traits in the Brazilian Cerrado, *Agric. For. Meteorol.*, 308,  
782 108551, <https://doi.org/10.1016/j.agrformet.2021.108551>, 2021b.

783 Turpault, M.P., Kirchen, G., Calvaruso, C., Redon, P.O., and Dincher, M.: Exchanges of major elements  
784 in a deciduous forest canopy, *Biogeochemistry*, 152, 51–71, [https://doi.org/10.1007/s10533-020-](https://doi.org/10.1007/s10533-020-00732-0)  
785 00732-0, 2021.

786 Wu, T., Song, Y.T., Tissue, D., Su, W., Luo, H.Y., Li, X., Yang, S.M., Liu, X.J., Yan J.H., Huang, J., and  
787 Liu, J.X.: Photosynthetic and biochemical responses of four subtropical tree seedlings to reduced  
788 dry season and increased wet season precipitation and variable N deposition, *Tree Physiol.*, 44(1),  
789 tpad114, <https://doi.org/10.1093/treephys/tpad114>, 2023.

790 Wu, Y.P., Yin, X.W., Zhou, G.Y., Bruijnzeel, L. A., Dai, A.G., Wang, F., Gentine, P., Zhang, G.C., Song,  
791 Y.N., and Zhou, D.C.: Rising rainfall intensity induces spatially divergent hydrological changes  
792 within a large river basin, *Nat. Commun.*, 15(1), 823, <https://doi.org/10.1038/s41467-023-44562-8>,  
793 2024.

794 Van Stan II, J.T., and Pypker, T.G.: A review and evaluation of forest canopy epiphyte roles in the  
795 partitioning and chemical alteration of precipitation, *Sci. Total Environ.*, 536, 813–824,  
796 <https://doi.org/10.1016/j.scitotenv.2015.07.134>, 2015.

797 Van Stan, J.T., Wagner, S., Guillemette, F., Whitetree, A., Lewis, J., Silva, L., and Stubbins, A.: Temporal  
798 dynamics in the concentration, flux, and optical properties of tree-derived dissolved organic matter  
799 in an epiphyte-laden oak-cedar forest, *J. Geophys. Res-Bioge.*, 122(11), 2982–2997.  
800 <https://doi.org/10.1002/2017JG004111>, 2017.

801 Wang, C.Y., Sun, X.C., Fan, C.B., Wei, Y.X., Jia, G.K., and Cao, Y.H.: Spatio-temporal variability and  
802 intra-event variation of throughfall ammonium and nitrate in a pine plantation, *Hydrol. Process.*, 37,  
803 e14872, <https://doi.org/10.1002/hyp.14872>, 2023.

804 Yan, J.H., Zhou, G.Y., Zhang, D.Q., and Wang, X.: Spatial and temporal variations of some hydrological  
805 factors in a climax forest ecosystem in the Dinghushan region, *Acta Ecol. Sin.*, 23(11), 2359–2366,  
806 <https://europepmc.org/article/cba/534217>, 2003.

807 Yue, K., De Frenne, P., Fornara, D.A., Van Meerbeek, K., Li, W., Peng, X., Ni, X.Y., Peng, Y., Wu, F.Z.,  
808 Yang Y.S., and Peñuelas, J.: Global patterns and drivers of rainfall partitioning by trees and  
809 shrubs, *Global Change Biol.*, 27(14), 3350–3357, <https://doi.org/10.1111/gcb.15644>, 2021.

810 Zabret, K., Rakovec, J., and Šraj, M.: Influence of meteorological variables on rainfall partitioning for  
811 deciduous and coniferous tree species in urban area, *J. Hydrol.*, 558, 29–41,  
812 <https://doi.org/10.1016/j.jhydrol.2018.01.025>, 2018.

813 Zhang, W.J., Zhu, X.A., Chen, C.F., Zeng, H.H., Jiang, X.J., Wu, J.E., Zou, X., Yang, B., and Liu, W.J.:  
814 Large broad-leaved canopy of banana (*Musa nana* Lour.) induces dramatically high spatial–  
815 temporal variability of throughfall, *Hydrol. Res.*, 52(6), 1223–1238,  
816 <https://doi.org/10.2166/nh.2021.023>, 2021.

817 Zhang, Y.F., Wang, X.P., Hu, R., Pan, Y.X., and Paradeloc, M.: Rainfall partitioning into throughfall,  
818 stemflow and interception loss by two xerophytic shrubs within a rain-fed re-vegetated desert  
819 ecosystem, northwestern China, *J. Hydrol.*, 527, 1084–1095,  
820 <https://doi.org/10.1016/j.jhydrol.2015.05.060>, 2015.



821 Zhang, Y.F., Yuan, C., Chen, N., and Levia, D.F.: Rainfall partitioning by vegetation in China: A  
822 quantitative synthesis, *J. Hydrol.* 617, 128946, <https://doi.org/10.1016/j.jhydrol.2022.128946>, 2023.

823 Zhao, W.Y., Ji, X.B., Jin, B.W., Du, Z.Y., Zhang, J.L., Jiao, D.D., and Zhao, L.W.: Experimental  
824 partitioning of rainfall into throughfall, stemflow and interception loss by *Haloxylon ammodendron*,  
825 a dominant sand-stabilizing shrub in northwestern China, *Sci. Total Environ.*, 858, 159928,  
826 <https://doi.org/10.1016/j.scitotenv.2022.159928>, 2023.

827 Zheng, M.H., Zhang, T., Luo, Y.Q., Liu, J.X., Lu, X.K., Ye, Q., Wang, S.H., Huang, J., Mao, Q.G., Mo,  
828 J.M., and Zhang, W.: Temporal patterns of soil carbon emission in tropical forests under long-term  
829 nitrogen deposition, *Nat. Geosci.*, 15, 1002–1010, <https://doi.org/10.1038/s41561-022-01080-4>,  
830 2022.

831 Zhou, G.Y., Wei, X.H., Wu, Y.P., Liu, S.G., Huang, Y.H., Yan, J.H., Zhang, D.Q., Zhang, Q.M., Liu, J.X.,  
832 Meng, Z., Wang, C.L., Chu, G.W., Liu, S.Z., Tang, X.L., and Liu, X.D.: Quantifying the  
833 hydrological responses to climate change in an intact forested small watershed in Southern China,  
834 *Global Change Biol.*, 17(12), 3736–3746, <https://doi.org/10.1111/j.1365-2486.2011.02499.x>, 2011.

835 Ziegler, A.D., Giambelluca, T.W., Nullet, M.A., Sutherland, R.A., Tantasarin, C., Vogler, J.B., and  
836 Negishi, J.N.: Throughfall in an evergreen-dominated forest stand in Northern Thailand: comparison  
837 of mobile and stationary methods, *Agric. For. Meteorol.*, 149, 373–384,  
838 <https://doi.org/10.1016/j.agrformet.2008.09.002>, 2009.

839 Zimmermann, A., Wilcke, W., and Elsenbeer, H.: Spatial and temporal patterns of throughfall quantity  
840 and quality in a tropical montane forest in Ecuador, *J. hydrol.*, 343(1–2), 80–96,  
841 <https://doi.org/10.1016/j.jhydrol.2007.06.012>, 2007.

842 **Tables**

843

844 **Table 1.** Correlations between throughfall and stemflow and rainfall and forest factors

	Gross rainfall	DBH	CA	Height	LAI
Throughfall	0.72***	—	—	—	-0.58**
stemflow	0.77***	0.65*	-0.75**	0.54**	-0.55**

845 DBH: diameter at breast height; CA: crown area; LAI: leaf area index. \* $P < 0.05$ , \*\* $P < 0.01$ , \*\*\* $P <$

846 0.001

847

848

849

850

851

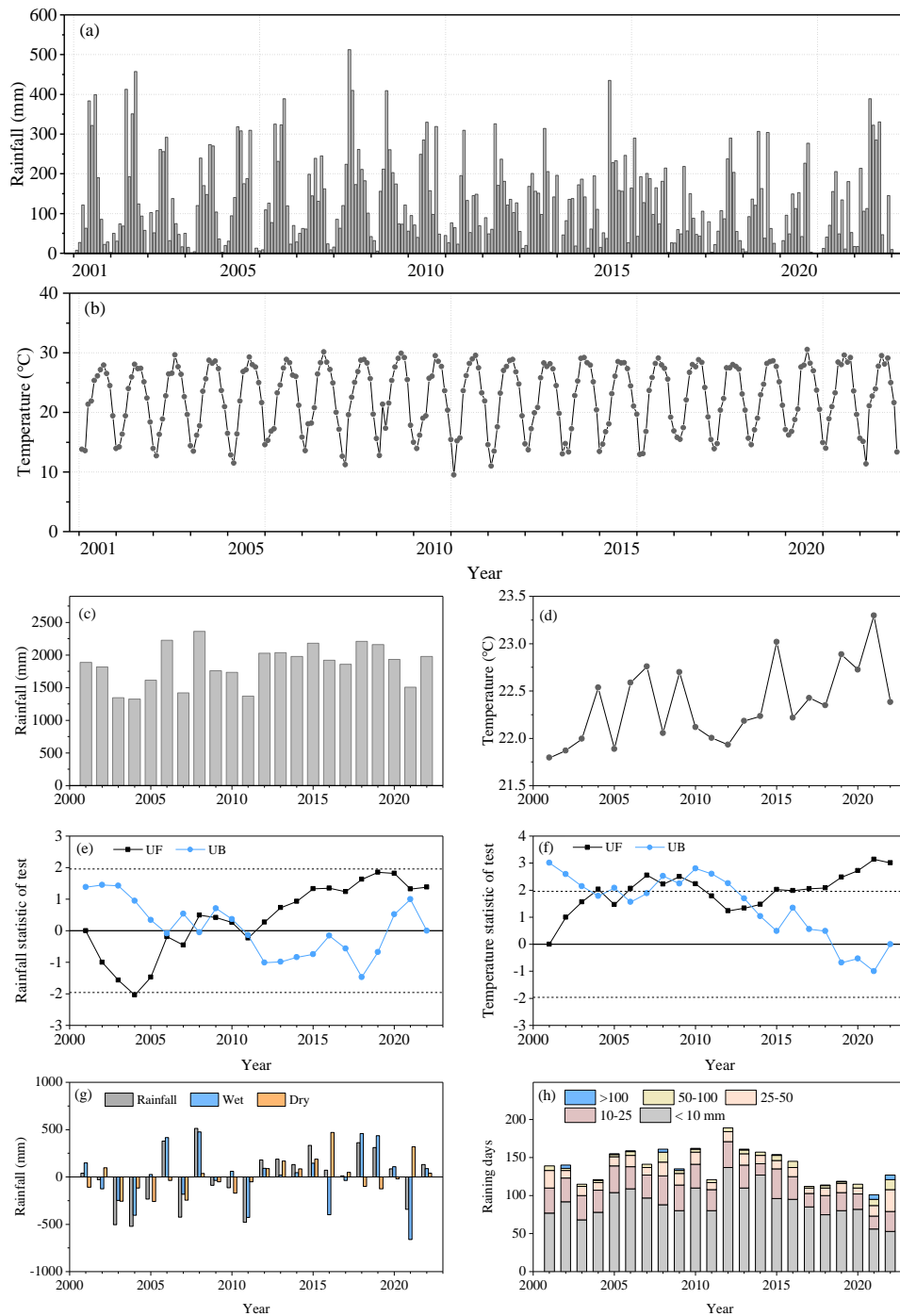
852

853 **Table 2.** Analysis of variance (ANOVA) for throughfall and stemflow affected by rainfall  
854 classifications and tree species

Summary of ANOVA	Throughfall		Stemflow
Rainfall classification (R)	< 0.05	Rainfall classification (R)	< 0.001
Forest type (F)	< 0.001	Tree species (T)	< 0.001
R × F	0.861	R × T	< 0.001

855  $\alpha = 0.05$

856



858

859 **Figure 1.** (a) and (b) rainfall and temperature in Dinghushan Biosphere Reserve in Southern China

860

861 from 2001–2022, (c) and (d) annual rainfall and temperature, (e) and (f) rainfall and

862

863 temperature statistic of Mann-Kendall test, respectively. (g) Anomaly of annual rainfall from

864

865 2001–2022, (h) annual raining days in five classifications. UF (Unadjusted Forward) > 0

866

867 indicate a continuous increasing trend ( $P < 0.05$ ). The intersection points of UF and UB

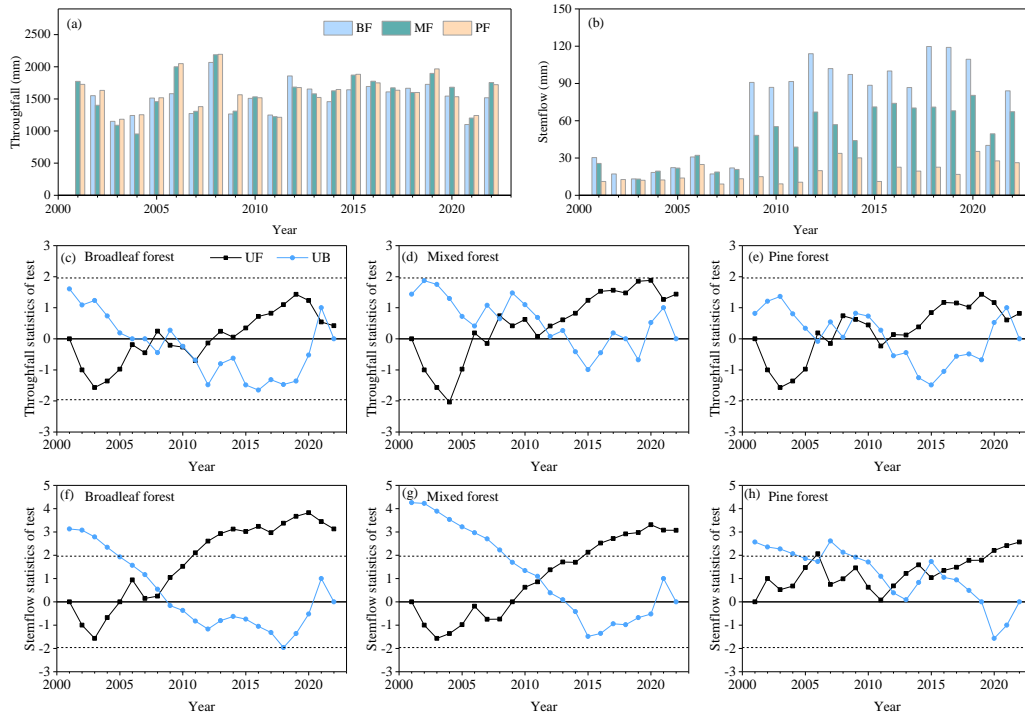
868

869 (Unadjusted Backward) is the mutation time point. Within the confidence interval [-1.96, 1.96],

870

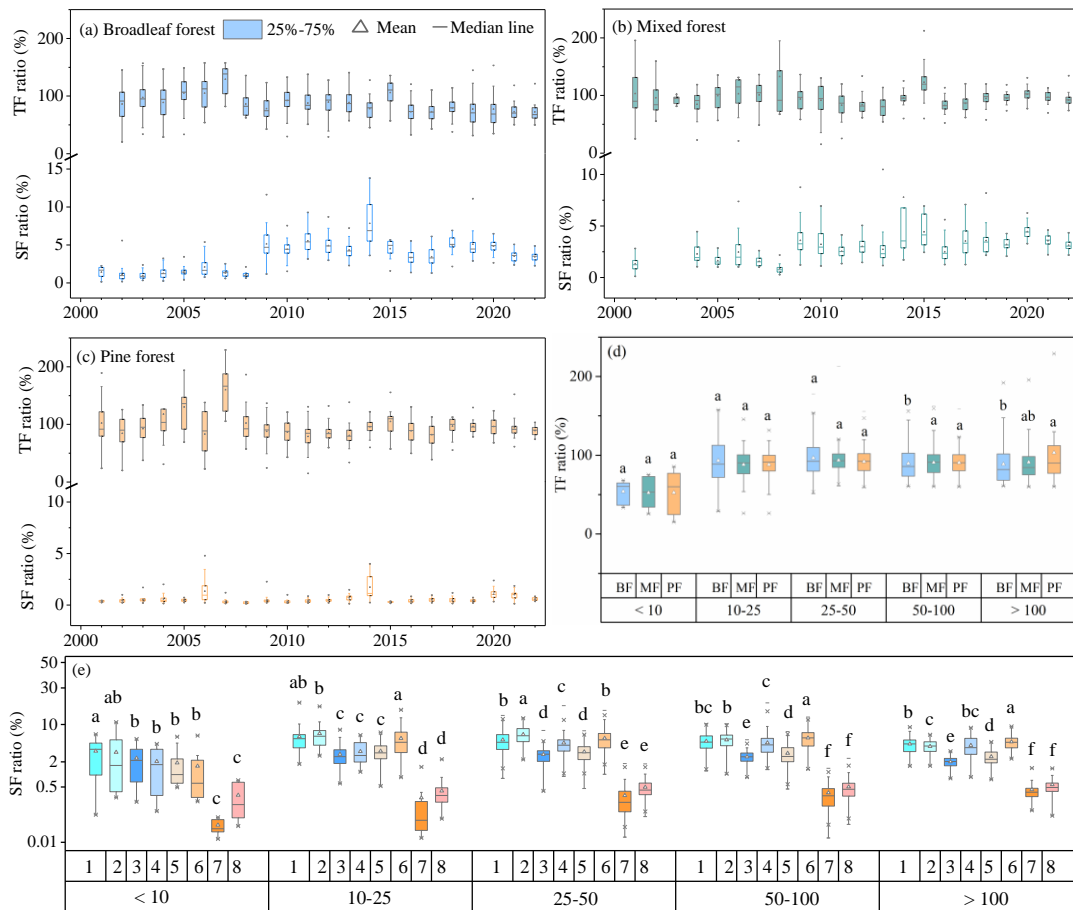
871 the variable presents a significantly mutation growth state at this time point ( $P < 0.05$ ).

872

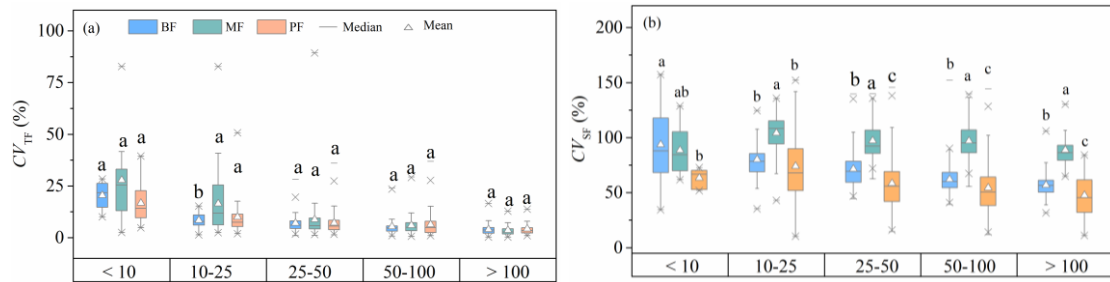


867

868 **Figure 2.** (a) and (b) Annual throughfall and stemflow in the broadleaf forest (BF), mixed pine and  
 869 broadleaf forest (MF) and pine forest (PF) from 2001–2022, respectively, (c) ~ (h) rainfall and  
 870 stemflow statistic of Mann-Kendall test, respectively. UF (Unadjusted Forward)  $> 0$  indicate a  
 871 continuous increasing trend ( $P < 0.05$ ). The intersection points of UF and UB (Unadjusted  
 872 Backward) is the mutation time point. Within the confidence interval  $[-1.96, 1.96]$ , the variable  
 873 presents a significantly mutation growth state at this time point ( $P < 0.05$ ).



874  
875 **Figure 3.** Box plots of throughfall ratio and stemflow ratio in (a) broadleaf forest, (b) mixed pine  
876 and broadleaf forest and (c) pine forest from 2001–2022. Boxed plots of (d) TF ratio in the  
877 three forests and (e) SF ratio for eight plant species based on the rainfall classifications  
878 (broadleaf forest: *Acmena acuminatissima* (Blume) Merr. et Perry (SF1), *Cryptocarya*  
879 *chinensis* (Hance) Hemsl. (SF2), *Girroniera subaequalis* Planch. (SF3), *Schima*  
880 *superba* Gardn. et Champ. (SF4); mixed forest: *Castanea henryi* (Skam) Rehd. et Wils. (SF5),  
881 *Schima superba* Gardn. et Champ. (SF6), *Pinus massoniana* Lamb. (SF7); pine forest: *Pinus*  
882 *massoniana* Lamb. (SF8). Different letters indicate a significant difference at  $P < 0.05$



884

885

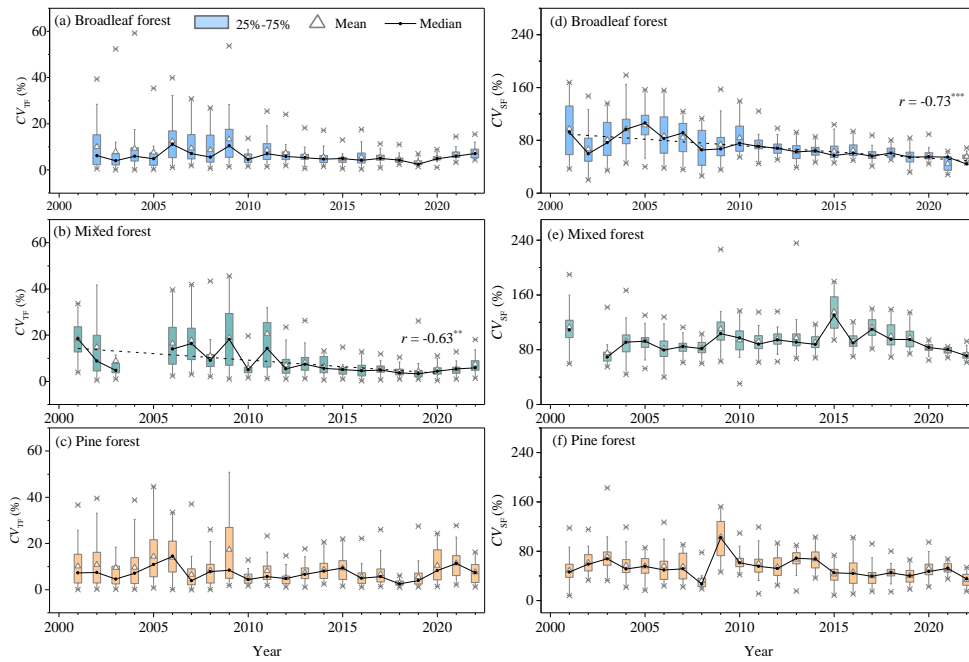
**Figure 4.** Box plots of coefficient of variation ( $CV$ , %) in (a) throughfall (TF) and (b) stemflow (SF)

886

in broadleaf forest (BF), mixed pine and broadleaf forest (MF) and pine forest (PF) based on

887

the rainfall classifications. Different letters indicate a significant difference at  $P < 0.05$



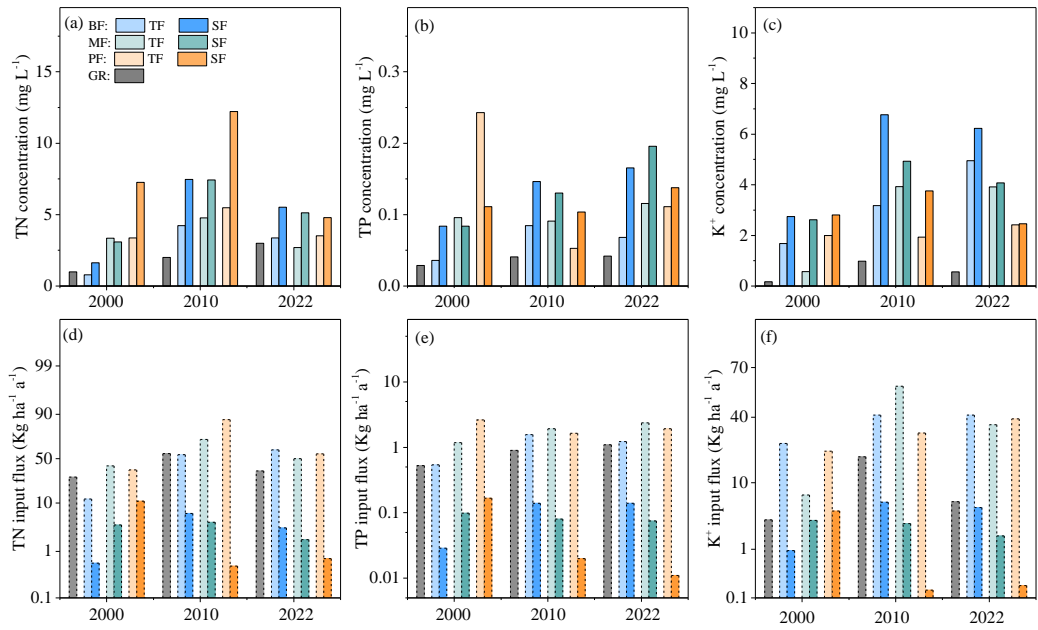
889

890

891

892

**Figure 5.** Box plots of coefficient of variation ( $CV$ , %) in (a, b, and c) throughfall (TF) and (d, e, and f) stemflow (SF) in the three forests from 2001 to 2022. Medians of annual  $CV$  were fitted.  $r$ : Pearson coefficient of correlation; \*:  $P < 0.05$ , \*\*:  $P < 0.01$ , \*\*\*:  $P < 0.001$



893

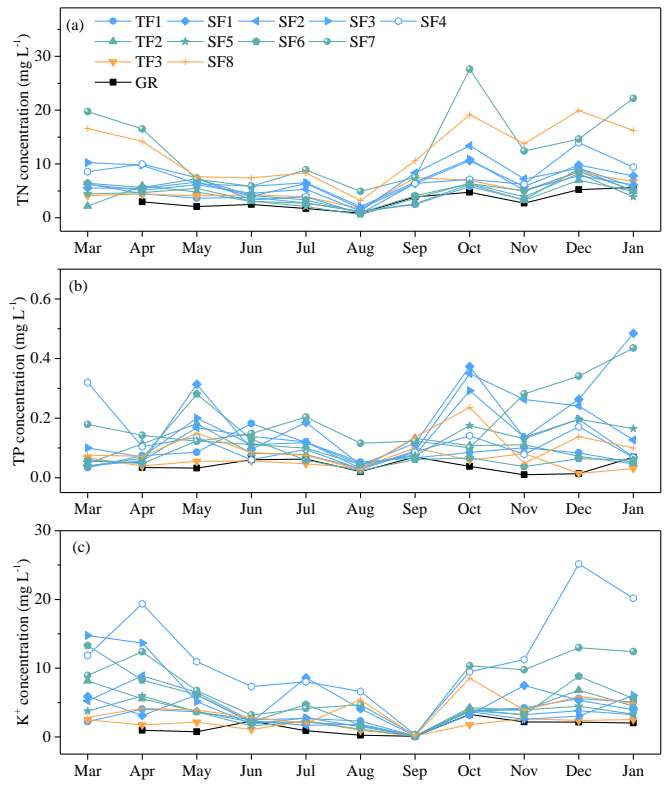
894

**Figure 6.** Concentrations and fluxes of TN, TP and K<sup>+</sup> of gross rainfall (GR), throughfall (TF) and stemflow (SF) in the broadleaf forest (BF), mixed forest (MF) and pine forest (PF) in 2000, 2010 and 2022, respectively.

895

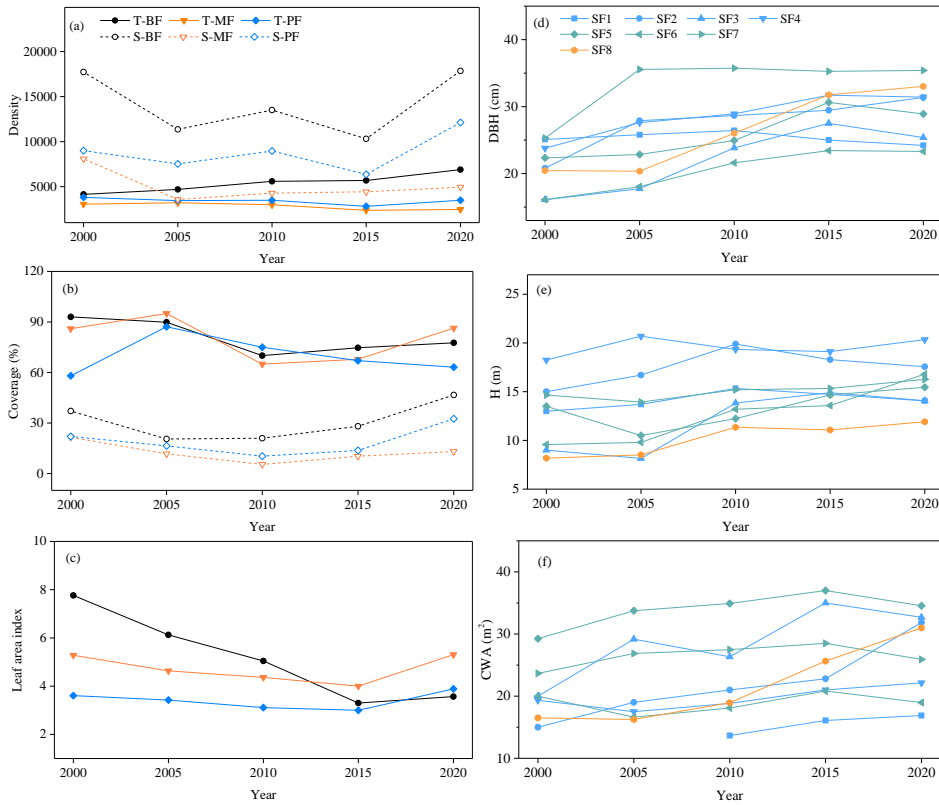
896





897  
 898  
 899  
 900

**Figure 7.** Monthly concentrations of (a) TN, (b) TP and (c) K<sup>+</sup> of throughfall (TF1) and stemflow (SF1, SF2, SF3 and SF4) in the broadleaf forest, throughfall (TF2) and stemflow (SF5, SF6 and SF7) in the mixed forest, throughfall (TF3) and stemflow (SF8) in the pine forest.



901 **Figure 8.** Plant density, canopy coverage and leaf area index of tree (T) and shrub (S) in the  
 902 broadleaf forest (BF), mixed forest (MF) and pine forest (PF), respectively. Diameter at breast  
 903 height (DBH), height (H) and crown area (CA) is given for eight stemflow-sampled trees,  
 904 respectively. Tree height was measured using laser range finder. Tape measure was used  
 905 to measure the diameter of trees at a height of 1.3 m, namely DBH (diameter at breast height).  
 906 CA (crown area): the laser rangefinder was used to measure the maximum diameter at the edge  
 907 of the canopy, with multiple measurements at different points to ensure accuracy. Plant density:  
 908 25 plots of 20 m × 20 m (A1-A25 plots) were built on a plot of 1hm<sup>2</sup> to survey tree density.  
 909 Then, 25 plots of 5 m × 5 m (B1-B25 plots) were randomly set on the A1-A25 plots to survey  
 910 shrub density. Finally, 25 plots of 1 m × 1 m (C1-C25 plots) were randomly set on the B1-B25  
 911 plots to survey herb density. Canopy coverage: 25 observation plots (1 m × 1 m) were selected  
 912 in the 1 hm<sup>2</sup> area of each forest type. The percentage of the surface area covered by plants to  
 913 the total plot area is termed canopy coverage (%). LAI (Leaf area index) was measured using  
 914 a LAI-2200 plant canopy analyzer with 90° view caps (Li-Cor Inc., USA). 10 observation  
 915 points (distance about 10 m) were selected in the 1 hm<sup>2</sup> area of each forest type with 5  
 916 replications.  
 917  
 918